



CrossMark
 click for updates

Cite this: *RSC Adv.*, 2015, 5, 38830

The effect of submicron bioactive glass particles on *in vitro* osteogenesis

Shaoqing Liu,^a Weiyu Gong,^a Yanmei Dong,^{*a} Qing Hu,^b Xiaofeng Chen^b and Xuejun Gao^a

This study investigated the effects of novel submicron bioactive glass (sm-BG) particles on *in vitro* osteogenesis and compared them to those of microscale bioactive glass (m-BG) particles. The ability of sm-BG particles to generate precipitates on their surface in the presence of simulated body fluid (SBF) was examined, and the effect of sm-BG particles on *in vitro* osteogenesis was evaluated by culturing human osteoblast-like osteosarcoma (MG-63) cells on particle-coated plates. It was found that sm-BG induced formation of precipitates after incubation for 24 hours in SBF. Compared with m-BG, sm-BG particles better promoted MG-63 cell adhesion and they induced expression of the *ALP*, *RUNX2* and *COL1* genes at an earlier stage and to a greater degree. This study demonstrates that submicron bioactive glass particles possess a high capacity for precipitates formation in SBF and improved osteogenic properties when compared to microscale BG particles.

Received 3rd March 2015
 Accepted 21st April 2015

DOI: 10.1039/c5ra03786g

www.rsc.org/advances

Introduction

Bioactive glass (BG) is an osteogenic material that shows high osteoconductivity and osteoinductivity. Conventionally, BG particles are used in the treatment of congenital and tumor-induced bone defects. In addition, they are also used as filler materials in a polymeric matrix to improve the structural properties and bioactivity of the matrix.^{1,2}

After BG contacts with physiological fluids, a layer of hydroxyapatite (HA) forms on its surface and this can bond with host bone.³ Furthermore, the dissolution products of BG, especially soluble ions of silicon and calcium, can up-regulate osteogenic gene expression in osteoblasts and induce rapid bone regeneration.⁴⁻⁶ The bioactivity of BG particles is greatly affected by their physical features.

The physical features of BG, including shape, particle diameter, degree of dispersion can affect the specific surface area of BG, and then affect its ions dissolution rate and bioactivity. Previous studies have shown that BG particles (molar composition: 80% SiO₂, 16% CaO, 4% P₂O₅) with regular spherical shape possess better biological properties compared to those with irregular shape.⁷ BG with smaller particle diameter and better degree of dispersion has larger specific area, which leads to faster precipitation of HA on the particle surface.⁸ Nanometer-sized 58S BG (molar composition: 60%

SiO₂, 36% CaO, 4% P₂O₅) was found to be more effective than micrometer-sized 58S BG in up-regulating osteogenic gene expression.⁹ Therefore, BG particles with regular shape, nanometer-size and good degree of dispersion will possess better bioactivity.

For BG fabricated by sol-gel process, pH in the preparing process is an important factor affecting physical features of the particles. The acid-catalyzed sol-gel process BG particles usually show irregular granular or blocky shape consisting of agglomerated nanoparticles,¹⁰ while alkali-catalyzed sol-gel BG particles possess good dispersion.¹¹ However, it is a challenge to fabricate particles with nanometer-sizes and incorporate calcium into the composition in the alkali-catalyzed sol-gel process.¹² Many researchers used acid-alkali catalyzed sol-gel process for the purpose of improving spherical morphology and degree of dispersion of traditional acid-catalyzed BG, and they synthesized BG with diameters smaller than 100 nm, like BG nanoparticles (molar composition: 58% SiO₂, 37% CaO, 5% P₂O₅) reported by Fan *et al.*¹³ and BG nanoparticales (molar composition: 55% SiO₂, 40% CaO, 5% P₂O₅) reported by Hong *et al.*,¹⁴ but the BG particles were not mono-dispersed or spherical shaped. Tsigkou¹⁵ synthesized mono-dispersed spherical BG particles (molar composition: 80% SiO₂, 20% CaO) with diameters of 215 ± 20 nm by alkali-catalyzed sol-gel process. They found the BG particles had no cytotoxicity to human bone marrow and adipose-derived stem cells at lower concentrations of 50 μg ml⁻¹ and that small decrease in metabolic activity and total DNA of both cell types was observed at higher BG concentrations of 100 and 200 μg ml⁻¹. However, further study needs to be done about their effects on osteogenesis.

^aDepartment of Cariology and Endodontology, Peking University School and Hospital of Stomatology, 22 Zhongguancun Nandajie, Haidian District, Beijing 100081, People's Republic of China. E-mail: kqdongyanmei@bjmu.edu.cn; Fax: +86 10 6217 3402; Tel: +86 10 8219 5475

^bNational Engineering Research Center for Tissue Restoration and Reconstruction, South China University of Technology, Guangzhou 510640, People's Republic of China

By alkali-catalyzed sol-gel method using dodecylamine (DDA) as a catalyst and template agent, we fabricated 77S BG particles (molar composition: 80% SiO₂, 16% CaO, 4% P₂O₅) with good spherical shape and degree of dispersion.¹⁶ Particle diameters were controlled to 200–800 nm by adjusting the concentration of DDA, and the BG particles with diameter of 500 nm show the best spherical shape and mono-dispersion.¹⁶ Using the same method, we recently fabricated 58S BG particles, and little is known about the osteogenic properties of this novel mono-dispersed BG. The aim of this study was to evaluate the osteogenic properties of our novel submicron BG (sm-BG) particles by examining their effect on HA formation and by comparing their impact on *in vitro* adhesion, proliferation and differentiation of MG-63 cells (human osteoblast-like osteosarcoma) to that of microscale BG (m-BG) particles.

Materials and methods

Materials

Both the sm-BG and the m-BG particles were composed of 58% SiO₂, 33% CaO and 9% P₂O₅ (w/w); they were prepared by the National Engineering Research Center for Human Tissue Restoration and Reconstruction, South China University of Technology. sm-BG with particle size of approximately 500 nm was prepared by the alkali-catalyzed sol-gel method, and m-BG with particle size between 2 and 20 μm was prepared *via* the traditional acid-catalyzed sol-gel method.¹⁷

Characterization of sm-BG particles

The surface area and pore structure of the particles were measured *via* N₂ adsorption at 77.3 K (Nova 4200e, Quantachrome, Boynton Beach, FL, USA). The specific surface area of the particles was calculated from a Brunauer-Emmett-Teller plot of the adsorption-desorption isotherm using adsorption points in the P/P_0 range from 0.05 to 0.35 (NOVA Win software, Quantachrome, Boynton Beach, FL, USA). Pore volumes were obtained from the volumes of N₂ adsorbed at $P/P_0 = 0.99$ or thereabout. The pore size and pore size distribution were calculated by the Barrett-Joyner-Halenda (BJH) method. The surface elemental composition of sm-BG was evaluated using an energy-dispersive X-ray spectroscopy (EDX) attached to field-emission scanning electron microscopy (FE-SEM; S4800, JEOL, Tokyo, Japan). The particle size distributions of sm-BG were tested by Zetasizer Nano ZS (Nano ZS, Malvern Instruments Ltd, Malvern, Worcestershire, United Kingdom).

HA formation on sm-BG particles in SBF

The *in vitro* bioactivity of sm-BG was tested in simulated body fluid (SBF) as described by Kokubo *et al.*¹⁸ The particles were immersed in SBF at a concentration of 1 mg ml⁻¹ at 37 °C and pH 7.25. After 1, 3 and 7 days of incubation, the solution was removed, and the solids were washed with acetone and dried in air. The surface morphology of sm-BG before and after incubation was observed by FE-SEM; prior to microscopy, samples were coated with gold (5 min, 50 mTorr). Some of the particles that had been incubated for 1 day were suspended in ethanol

using a sonicator (SB-5200, Scientz Biotechnology Co., Ltd, Ningbo, China) before being collected on copper grids for assessment of HA formation by transmission electron microscopy (TEM; JEM-2100HR, JEOL, Tokyo, Japan).

Coating culture surfaces with m-BG and sm-BG particles

The m-BG and sm-BG particles were sterilized in a dry heat oven (DHG-9203A, Shanghai Yiheng technology co., Ltd, Shanghai, China) at 180 °C for 4 hours. Then they were suspended in deionized water respectively at a concentration of 0.1 mg ml⁻¹. The suspension was added to the wells of a 6-, 12-, 24- and 96-well polystyrene tissue culture plate (Costar, Cambridge, MA, USA), which were then dried under sterilized airflow. The suspension volume added to each culture plate well equals to the culture medium volume in cell experiment, that are 2 ml, 1 ml, 0.5 ml and 0.1 ml for 6-, 12-, 24- and 96-well culture plate, respectively. So the concentration of BG in cell experiment is 0.1 mg ml⁻¹. For the observation of cell adhesion by FE-SEM, the 0.1 mg ml⁻¹ suspension was added to a 24-well plate containing circular glass coverslips, which were then dried under sterilized airflow. In both cases, the BG particles adhered stably to the surfaces of the well floors or to the glass coverslips (Fig. 1).

MG-63 cell culture

Human osteoblast-like osteosarcoma (MG-63) cells were maintained in Dulbecco's Modified Eagle Medium (DMEM, Gibco, Gaithersburg, MD, USA) containing 10% FBS (Ausbone, Gold Coast, Queensland, Australia) and 100 U per mL penicillin per streptomycin (Sigma-Aldrich, St. Louis, MO, USA) in an incubator with a humidified atmosphere of 95% air and 5% CO₂ at 37 °C.

Adhesion of MG-63 cells

MG-63 cells were seeded at 5000 cells per well on circular glass coverslips coated with m-BG or sm-BG particles in 24-well plates. After culturing for 2 days, the MG-63 cells were observed under an inverted light microscope. Then they were fixed on the coverslips in 2.5% glutaraldehyde, and dehydrated *via* serial treatment with ethanol solutions of increasing concentration (50%, 70%, 80%, 90%, 95% and 100% v/v in water). After coating with gold (5 min, 50 mTorr), the interaction of the particles and MG-63 cells was observed by FE-SEM.

Proliferation of MG-63 cells

MG-63 cells were seeded at 3000 cells per well in 96-well plates coated with m-BG or sm-BG particles. Wells without the BG coating served as controls. Cell proliferation was measured using a cell counting kit-8 assay (CCK-8, Dojindo, Kumamoto, Japan) after culturing for 1, 3, 5, 7, 10 and 14 days. The optical density was measured *via* spectrophotometric absorbance at 450 nm using a 96-well microplate reader (BioTeK Instruments, Winooski, VT, USA).

Osteogenic-gene expression in MG-63 cells

The MG-63 cells were seeded in 6-well plates coated with m-BG or sm-BG particles, or uncoated. At days 2, 4, and 7, the total

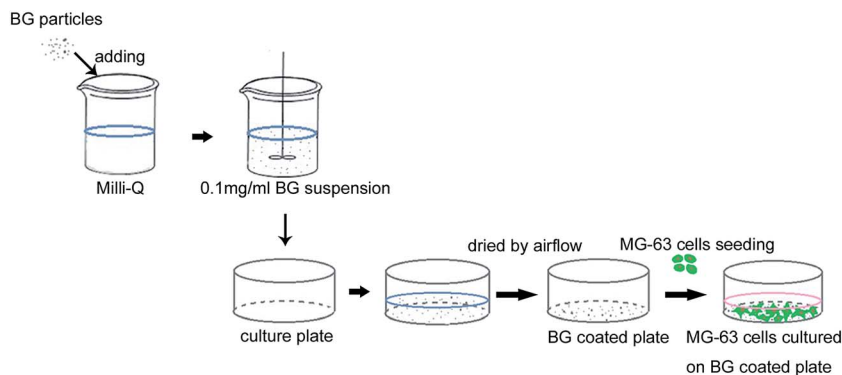


Fig. 1 Schematic representation of procedure for cell experiments.

RNA was extracted using TRIzol (Invitrogen, Carlsbad, CA, USA) according to the manufacturer's instructions. cDNA was then synthesized from 2 μg of total RNA with M-MLV reverse transcriptase (Promega, Madison, WI, USA) according to the manufacturer's instructions. Real-time (quantitative) reverse transcription-polymerase chain reaction (qRT-PCR) was performed using the FastStart Universal SYBR Green PCR Master mix (Roche, Basel, Switzerland) and an ABI 7500 thermal cycler (Applied Biosystems, Foster City, CA, USA). The sequences of the primer sets used to detect alkaline phosphatase (*ALP*), collagen I (*COL1*), runt-related transcription factor 2 (*RUNX2*), osteocalcin (*OCN*) and glyceraldehyde-3-phosphate dehydrogenase (*GAPDH*) are listed in Table 1. The qRT-PCR conditions were as follows: 50 $^{\circ}\text{C}$ for 2 min, 95 $^{\circ}\text{C}$ for 10 min, followed by 40 cycles at 95 $^{\circ}\text{C}$ for 15 s and 60 $^{\circ}\text{C}$ for 1 min. The housekeeper gene, *GAPDH* was used as an internal control. Gene expression was described as fold changes relative to the control group (uncoated wells) at day 2.

ALP activity in MG-63 cells

The MG-63 cells were seeded at 50 000 cells per well in 12-well plates and cultured for 7 or 14 days; wells were coated with m-BG or sm-BG, or were left as uncoated controls. ALP activity was determined using an alkaline phosphatase assay kit (Nanjing Jiancheng Technological Inc, Nanjing, China). The optical density was recorded at 520 nm using a 96-well microplate reader. A standard curve of known concentrations was

generated concurrently, and the protein concentrations were determined using the BCA protein assay (Pierce, Rockford, IL, USA). ALP activity was expressed per gram of protein.

Statistical analysis

Each result was the average of at least three independent experiments. Datas are reported as mean \pm standard deviation (SD). Comparisons between groups were analyzed by Student's *t*-test or one way ANOVA, using SPSS software (version 13.0, SPSS Inc., Chicago, IL, USA). Differences were considered significant at $p < 0.05$.

Results

Characterization of sm-BG particles

The specific surface area and mesopore structure of sm-BG particles were obtained from N_2 adsorption-desorption isotherms (Fig. 2a). The specific surface area, total pore volume and mean mesopore size of the sm-BG particles were $38.087 \pm 0.1 \text{ m}^2 \text{ g}^{-1}$, $0.382 \pm 0.01 \text{ cm}^3 \text{ g}^{-1}$ and $4.015 \pm 0.03 \text{ nm}$, respectively. In addition, sm-BG particles had a narrow pore-size distribution, mainly in the range of 2 to 5 nm (Fig. 2b). The corresponding data for m-BG was reported in our previous work, which were $28.020 \pm 0.1 \text{ m}^2 \text{ g}^{-1}$, $0.113 \pm 0.01 \text{ cm}^3 \text{ g}^{-1}$ and $15.504 \pm 0.02 \text{ nm}$.¹⁷ Compared to m-BG, sm-BG particles had a larger specific surface area and total pore volume, and a smaller average mesopore size. The EDX spectra showed that the surface

Table 1 The primer sequences used for real-time reverse transcription-polymerase chain reaction

Target gene	Primer sequence (5' to 3')	Product size (bp)
<i>ALP</i>	Forward: 5'-AGCACTCCCACTTCATCTGGAA-3' Reverse: 5'-GAGACCCAATAGGTAGTCCACATTG-3'	77
<i>COL1</i>	Forward: 5'-CGAAGACATCCCACCAATCAC-3' Reverse: 5'-TGTCGCAGACGCAGAT-3'	98
<i>RUNX2</i>	Forward: 5'-ACCCAGAAGGCACAGACAGAAG-3' Reverse: 5'-AGGAATGCGCCCTAAATCACT-3'	82
<i>OCN</i>	Forward: 5'-AGGGCAGCGAGGTAGTGA-3' Reverse: 5'-CCTGAAAGCCGATGTGGT-3'	150
<i>GAPDH</i>	Forward: 5'-CAACGGATTGGTCTGATTGG-3' Reverse: 5'-GCAACAATATCCACTTTACCAGAGTTAA-3'	72

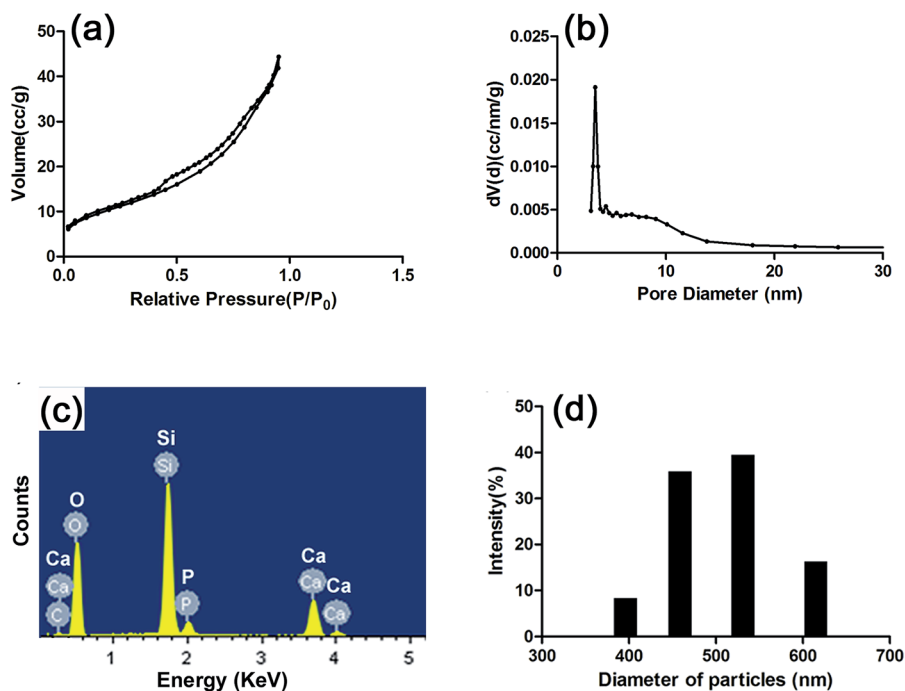


Fig. 2 Characterization of sm-BG. N₂ adsorption–desorption isotherms (a) and the mesopore size distributions (b) of sm-BG by N₂ adsorption experiments; (c) surface element composition of sm-BG by energy-dispersed X-ray spectroscopy; (d) particle size distributions of sm-BG by Zetasizer Nano-ZS.

elements of the sm-BG were silicon, calcium, phosphorus and oxygen; the semi-quantitative analyze showed the molar composition of sm-BG were 69% SiO₂, 23.1% CaO and 7.9% P₂O₅ (Fig. 2c). The Zetasizer Nano ZS showed the average particle diameters of sm-BG were 507.6 ± 63.2 nm (Fig. 2d). In our previous study, we reported the size of m-BG (molar composition: 60% SiO₂, 36% CaO, 4% P₂O₅) were between 2 and 20 μm .¹⁷

HA formation on sm-BG particles in SBF

FE-SEM and TEM of HA formation on sm-BG is shown in Fig. 3. Prior to immersion in SBF, sm-BG particles exhibited regular spherical morphology, rough surfaces, and diameters of approximately 500 nm (Fig. 3a). After 1 day in SBF, some lamellar deposits formed between the particles (Fig. 3b). Furthermore, TEM revealed the presence of rod-shaped crystals on the surface of the particles (Fig. 3b, insert). After 3 days, porous deposits appeared between the sm-BG particles, which decreased in size while increasing their surface roughness (Fig. 3c). After 7 days, a layer of porous deposits covered the surface of the particles (Fig. 3d). This clearly demonstrates the occurrence of a dynamic process whereby the BG dissolved and a surface layer of deposits formed.

Effect of sm-BG particles on adhesion of MG-63 cells

The adhesion of MG-63 cells on glass coverlips coated with sm-BG and m-BG particles was assessed *via* light microscopy and FE-SEM (Fig. 4). It was found that sm-BG particles were more evenly distributed on the glass substrate than m-BG (Fig. 4a and b). MG-63 cells were uniformly distributed in the sm-BG group (Fig. 4d) and covered by sm-BG particles (Fig. 4f). In contrast, MG-

63 cells tended to grow around m-BG clusters (Fig. 4c). MG-63 filopodia spread out and surrounded the particles to a greater degree in the sm-BG group (Fig. 4g and h). In both BG groups, the cells maintained their characteristic morphology (Fig. 4c and d).

Effect of sm-BG particles on proliferation of MG-63 cells

The effect of sm-BG and m-BG particles on MG-63 proliferation as evaluated by CCK-8 assay is shown in Fig. 5. The optical density (OD) values for the sm-BG and m-BG groups were

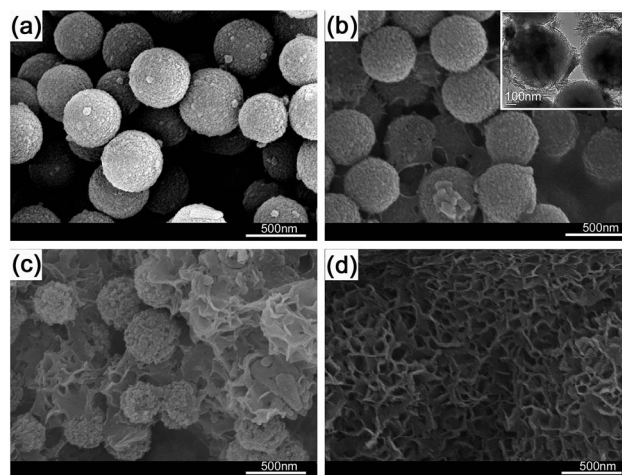


Fig. 3 Representative FE-SEM images of the surface morphology of sm-BG before (a) and after immersion in SBF for 1 day (b), 3 days (c) and 7 days (d). Insert of (b) shows TEM image of sm-BG morphology after immersion in SBF for 1 day.

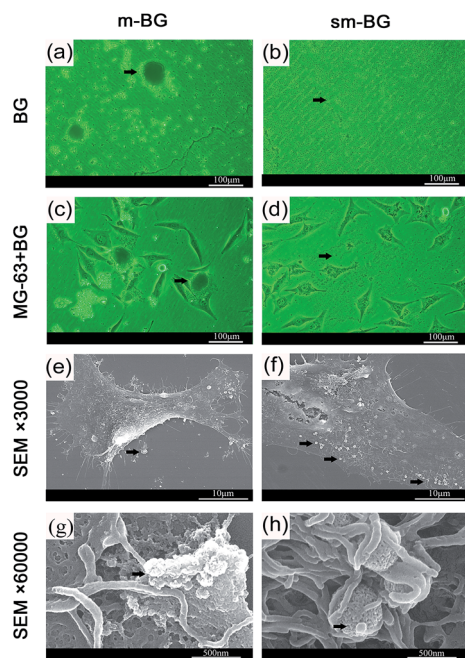


Fig. 4 Effects of submicron and microscale bioactive glass (sm-BG, m-BG) particles on the adhesion of MG-63 cells. Representative light microscope images showing distribution of BG particles coated on the culture dish (a and b) and MG-63 cells cultured with BG particles (c and d). Representative FE-SEM images of MG-63 cells cultured with m-BG and sm-BG (e–h). Arrows represents BG particles.

similar to those for the control group. The only significant change was at day 7, where the OD was higher for the sm-BG group than for that of the control group and m-BG group ($p < 0.05$); the m-BG group did not differ from controls at this or any other time point ($p > 0.05$).

Effect of sm-BG particles on the osteogenic differentiation of MG-63 cells

mRNA expression for the osteogenic marker genes, *ALP*, *RUNX2*, *COL1* and *OCN* in MG-63 cells cultured in BG-coated wells is shown in Fig. 6a–d. Compared with the control group, expression of *ALP*, *RUNX2* and *COL1* was up-regulated in both BG groups. sm-BG particles induced up-regulation of *ALP* expression on days 2, 4 and 7 ($p < 0.05$), *RUNX2* on days 4 ($p < 0.05$) and *COL1* on days 4 and 7 ($p < 0.05$). However, *ALP*, *RUNX2* and *COL1* expression was only up-regulated by m-BG particles on day 7 ($p < 0.05$).

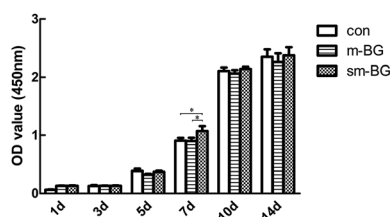


Fig. 5 Effects of submicron and microscale bioactive glass (sm-BG, m-BG) particles on the proliferation of MG-63 cells (CCK-8 assay). * $p < 0.05$.

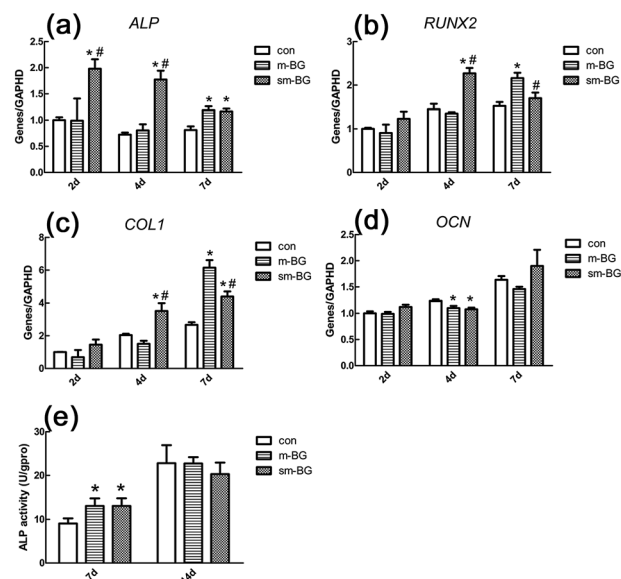


Fig. 6 Effects of submicron and microscale bioactive glass (sm-BG, m-BG) particles on osteogenic differentiation of MG-63 cells. Quantitative RT-PCR analysis of *ALP* (a), *RUNX2* (b), *COL1* (c) and *OCN* (d) gene expression in MG-63 cells cultured with sm-BG or m-BG particles. *ALP* (protein) activity in MG-63 cultured with sm-BG or m-BG particles (e). *Significant difference between the m-BG or sm-BG group and the control group ($p < 0.05$). #Significant difference between the m-BG group and the sm-BG group ($p < 0.05$).

0.05). Up-regulation of *OCN* expression was not detected in either BG group.

The results of the *ALP* (protein) activity assay showed that this was significantly elevated in both BG groups on day 7 ($p < 0.05$). No difference was found between the two BG groups. On day 14, no significant difference was found among the BG and control groups (Fig. 6e).

Discussion

Our novel sm-BG particles, synthesized by the alkali-catalyzed sol-gel method, were approximately 500 nm in diameter and of regular spherical shape. And m-BG presented irregular structures, with sizes ranging between 2 and 20 μm .¹⁷ Both sm-BG and m-BG have nanopore structure on their surface. And the synthesis procedure for sm-BG is simpler than that of m-BG because of the omission of grinding and sieving of the fine m-BG powder, however, this method produces a relative low yield. Compared with monodispersed spherical BGs fabricated in early studies, sm-BG particles have relative big specific area and uniform particle size.^{7,19} The smaller size (500 nm) and regular shape of sm-BG meant that their specific surface area was increased over the larger (2–20 μm (ref. 17)), irregularly shaped m-BG particles, which were fabricated by an acid-catalyzed sol-gel process. Previous study has shown that acid-catalyzed sol-gel derived microscale BG exhibits improved bioactivity compared with melt derived BG, on account of its particular mesoporous structure and large specific surface area.¹⁰ This suggests that the physical characteristics of our sm-

BG particles could allow for further improvement of bioactivity and hence osteogenesis.

To test this hypothesis, we first looked at formation of HA which is similar to bone mineral, on the surface of BG when physiological fluids/media (e.g., SBF) are present. The ability of BG to bond to bone is attributed to this,³ so HA production capacity in SBF is a useful marker for predicting the *in vivo* osteogenic activity of BG.²⁰ In this study, we detected formation of rod-shaped precipitates on the sm-BG particles after 24 hours, which closely resembled the natural nanoscale hydroxyapatite crystal²¹ and were confirmed HA in our previous study;¹⁶ this demonstrates a high capacity for HA formation. This is consistent with the previous studies of bioactivity of other alkali-catalyzed sol-gel bioactive glass *in vitro*.¹⁹ The dynamic process of sm-BG dissolution and HA formation at the particle surface was clearly shown and this strongly supports the theory that surface dissolution and ion release occur as part of the HA formation process.³

Previous studies have shown that the surface properties of materials greatly influence the adhesion and differentiation of osteoblasts,^{8,22–24} so we used an *in vitro*, direct-contact model to examine the osteogenic effect of sm- and m-BG particles on MG-63 cells. Both BGs showed good compatibility with the cells, which is consistent with previous studies of bioglass particles in contact with other cell types.^{15,20} Filopodia are fine projections of the cell membrane that are very important for environmental sensing, cell spreading and cell adhesion.²⁵ In this study, the filopodia of MG-63 cells adhered to both sm-BG and m-BG particles, but they wrapped around the sm-BG particles more tightly and in greater numbers, indicating that sm-BG enhanced cell adhesion and compatibility, respectively.

In present study, neither sm-BG nor m-BG had any significant effect on the proliferation of MG-63 cells. Consistent with our study, Tsigkou *et al.*²² found that 45S5 conditioned medium with Si concentration of 15 or 20 mg ml⁻¹ didn't significantly affect the metabolic activity and growth of human fetal osteoblasts; also, Isaac *et al.*²⁶ found that B75 bioactive glass (73.7 mol% SiO₂ and 26.3 mol% CaO) at the concentration of 4 mg ml⁻¹ showed no significant effect on the viability and metabolic activity of mouse fetal osteoblasts. However, ionic extraction of 45S5, 58S and nano-scale 58S at the concentration of 1 mg ml⁻¹ were found to inhibit the proliferation of cultured human dental pulp cells;⁹ additionally, 58S bioactive glass with nanoscale surface morphology were considered to enhance the proliferation of rat marrow mesenchymal cells.²⁷ These diverse functions of BG on cell proliferation might be caused by different released ionic dissolution of the certain BG material, which further influenced the expression of proliferation-related genes.⁴ For example, 2~4 mM Ca was found to be suitable for osteoblasts proliferation, while higher concentrations with more than 10 mM Ca were cytotoxic.²⁸

The effect of sm-BG particles on differentiation of the osteoblast-like MG-63 cells was investigated *via* qRT-PCR, and important marker genes (*COL1*, *ALP*, *RUNX2*, *OCN*) representing different stages of osteoblast differentiation were analyzed. *COL1* is expressed during the initial period of proliferation and extracellular-matrix synthesis; it is the most abundant type of collagen in bone and acts as a structural matrix for mineral

deposition.²⁹ *ALP* is expressed during the post-proliferative period and is a marker of early differentiation and extracellular matrix mineralization.³⁰ *RUNX2* is a master transcription factor regulating osteogenesis and another indicator of early osteoblast differentiation.^{31,32} In our study, both sm-BG and m-BG showed promotive effects on the expression of *ALP*, *RUNX2* and *COL1* genes, consistent with previous observations that BG could enhance osteogenic gene expression.^{22,33} Particularly, we found that in sm-BG group, compared with m-BG group, the up-regulation of *ALP*, *RUNX2* and *COL1* was stronger and the onset was more rapidly. Since a large specific surface area was considered to increase the dissolution rate of ions, the larger specific surface area of sm-BG than m-BG might translate into an accelerated rate of ion dissolution.³⁴ Thus, the concentrations of Si and Ca in sm-BG group could reach the level necessary for osteogenesis earlier than m-BG, and hence enhanced and brought ahead the osteogenic differentiation of MG-63 cells. Consistent with this phenomenon, a previously published study³⁵ from our lab showed that compared with 45S5, the nano-scale 58S with larger specific area induced the differentiation and mineralization of MG-63 cells more efficiently. Besides, the surface morphology of a material can also affect cell differentiation. For example, nanophase surface could significantly enhance the osteogenic differentiation of osteoblasts cultured on it.³⁶ Furthermore, the osteogenic differentiation of human mesenchymal stromal cells (hMSC) was highly sensitivity affected by the topographic details.³⁷ In this study, sm-BG and m-BG were both with nanopore structure, and the sm-BG was regular spherical submicron particles, yet m-BG was irregular micron particles. This difference in the morphology of sm-BG and m-BG might be another reason of their different effects on MG-63 differentiation, which needs further investigation. In our study, the *ALP* and *RUNX2* gene expression were relatively high during the observation time points, indicating the MG-63 cells maybe mainly in the differentiation period. Since *OCN* usually denotes osteoblast maturation and the onset of matrix mineralization,³⁸ it showed no up-regulation during the observation time points. This pilot study of sm-BG on the *ALP* activity of MG-63 showed the promoting effect of sm-BG and m-BG at day 7, and no difference was observed between the two BG groups; therefore, further investigations on protein level is needed for more time points and more osteogenic markers in the future study. In conclusion, the promoting effect of our novel designed sm-BG on the gene expression of *ALP*, *RUNX2* and *COL1* suggests that the use of sm-BG particles may enhance and accelerate the early stages of osteogenesis over m-BG.

Conclusions

Submicron bioactive glass (sm-BG) particles were found to form rod-shaped precipitates after 24 hours of incubation in SBF. Compared with microscale particles (m-BG), sm-BG particles better promoted *in vitro* adhesion of osteoblast-like osteosarcoma (MG-63) cells, and they induced earlier and increased expression of the osteogenic marker genes, *ALP*, *RUNX2* and *COL1*. These results suggest that our novel sm-BG particles are

superior to conventionally acid-catalyzed sol-gel m-BG particles in terms of their capacity to enhance osteogenesis.

Acknowledgements

The authors are grateful for the support of the National Natural Science Foundation of China (no. 51372005).

Notes and references

- 1 A. Gantar, L. P. da Silva, J. M. Oliveira, A. P. Marques, V. M. Correlo, S. Novak and R. L. Reis, *Mater. Sci. Eng., C*, 2014, **43**, 27–36.
- 2 P. R. Gabbai-Armelin, D. Alves Cardoso, E. D. Zanotto, O. Peitl, S. C. G. Leeuwenburgh, J. A. Jansen, A. C. M. Renno and J. J. J. P. van den Beucken, *RSC Adv.*, 2014, **4**, 45778.
- 3 L. L. Hench, *J. Mater. Sci.: Mater. Med.*, 2006, **17**, 967–978.
- 4 I. D. Xynos, A. J. Edgar, L. D. Buttery, L. L. Hench and J. M. Polak, *J. Biomed. Mater. Res.*, 2001, **55**, 151–157.
- 5 L. L. Hench, *J. Eur. Ceram. Soc.*, 2009, **29**, 1257–1265.
- 6 J. R. Jones, *Acta Biomater.*, 2013, **9**, 4457–4486.
- 7 T. A. Ostomel, Q. Shi, C. K. Tsung, H. Liang and G. D. Stucky, *Small*, 2006, **2**, 1261–1265.
- 8 J. Zhong and D. C. Greenspan, *J. Biomed. Mater. Res.*, 2000, **53**, 694–701.
- 9 W. Gong, Z. Huang, Y. Dong, Y. Gan, S. Li, X. Gao and X. Chen, *J. Endod.*, 2014, **40**, 83–88.
- 10 J. Zhong and D. C. Greenspan, *J. Biomed. Mater. Res.*, 2000, **53**, 694–701.
- 11 Z. Hong, G. M. Luz, P. J. Hampel, M. Jin, A. Liu, X. Chen and J. F. Mano, *J. Biomed. Mater. Res.*, 2010, **95**, 747–754.
- 12 S. Lin, C. Ionescu, K. J. Pike, M. E. Smith and J. R. Jones, *J. Mater. Chem.*, 2009, **19**, 1276–1282.
- 13 J. P. Fan, P. Kalia, L. Di Silvio and J. Huang, *Mater. Sci. Eng., C*, 2014, **36**, 206–214.
- 14 Z. Hong, R. L. Reis and J. F. Mano, *J. Biomed. Mater. Res.*, 2009, **88**, 304–313.
- 15 O. Tsigkou, S. Labbaf, M. M. Stevens, A. E. Porter and J. R. Jones, *Adv. Healthcare Mater.*, 2014, **3**, 115–125.
- 16 Q. Hu, Y. Li, G. Miao, N. Zhao and X. Chen, *RSC Adv.*, 2014, **4**, 22678–22687.
- 17 S. Wang, X. Gao, W. Gong, Z. Zhang, X. Chen and Y. Dong, *Acta Biomater.*, 2014, **10**, 2792–2803.
- 18 T. Kokubo, H. Kushitani, S. Sakka, T. Kitsugi and T. Yamamuro, *J. Biomed. Mater. Res.*, 1990, **24**, 721–734.
- 19 S. Labbaf, O. Tsigkou, K. H. Muller, M. M. Stevens, A. E. Porter and J. R. Jones, *Biomaterials*, 2011, **32**, 1010–1018.
- 20 T. Kokubo and H. Takadama, *Biomaterials*, 2006, **27**, 2907–2915.
- 21 S. Wagner and H. D. Wagner, *Annu. Rev. Mater. Res.*, 1998, **28**, 271–298.
- 22 O. Tsigkou, J. R. Jones, J. M. Polak and M. M. Stevens, *Biomaterials*, 2009, **30**, 3542–3550.
- 23 V. G. Varanasi, J. B. Owyong, E. Saiz, S. J. Marshall, G. W. Marshall and P. M. Loomer, *J. Biomed. Mater. Res., Part A*, 2011, **98**, 177–184.
- 24 J. Mitra, G. Tripathi, A. Sharma and B. J. Basu, *RSC Adv.*, 2013, **3**, 11073–11094.
- 25 Y. Zhao, Y. Zhang, F. Ning, D. Guo and Z. Xu, *J. Biomed. Mater. Res., Part B*, 2007, **83**, 121–126.
- 26 J. Isaac, J. Nohra, J. Lao, E. Jallot, J. M. Nedelec, A. Berdal and J. M. Sautier, *Eur. Cells Mater.*, 2011, **21**, 130–143.
- 27 B. Lei, X. Chen, Y. Wang, N. Zhao, C. Du and L. Fang, *J. Biomed. Mater. Res., Part A*, 2010, **94**, 1091–1099.
- 28 S. Maeno, Y. Niki, H. Matsumoto, H. Morioka, T. Yatabe, A. Funayama, Y. Toyama, T. Taguchi and J. Tanaka, *Biomaterials*, 2005, **26**, 4847–4855.
- 29 S. K. Kim, H. Y. Park, Y. H. Jang, J. H. Lee and J. K. Kim, *Plant Sci.*, 2013, **199–200**, 71–78.
- 30 S. K. Misra, D. Mohn, T. J. Brunner, W. J. Stark, S. E. Philip, I. Roy, V. Salih, J. C. Knowles and A. R. Boccaccini, *Biomaterials*, 2008, **29**, 1750–1761.
- 31 T. Komori, H. Yagi, S. Nomura, A. Yamaguchi, K. Sasaki, K. Deguchi, Y. Shimizu, R. T. Bronson, Y. H. Gao, M. Inada, M. Sato, R. Okamoto, Y. Kitamura, S. Yoshiki and T. Kishimoto, *Cell*, 1997, **89**, 755–764.
- 32 T. Komori and T. Kishimoto, *Curr. Opin. Genet. Dev.*, 1998, **8**, 494–499.
- 33 G. Jell, I. Notingher, O. Tsigkou, P. Notingher, J. M. Polak, L. L. Hench and M. M. Stevens, *J. Biomed. Mater. Res., Part A*, 2008, **86**, 31–40.
- 34 M. Vollenweider, T. J. Brunner, S. Knecht, R. N. Grass, M. Zehnder, T. Imfeld and W. J. Stark, *Acta Biomater.*, 2007, **3**, 936–943.
- 35 W. Gong, Y. Dong, X. Chen and B. Karabucak, *Chin. J. Dent. Res.*, 2012, **15**, 145–152.
- 36 T. J. Webster, C. Ergun, R. H. Doremus, R. W. Siegel and R. Bizios, *Biomaterials*, 2000, **21**, 1803–1810.
- 37 J. Fiedler, B. Ozdemir, J. Bartholoma, A. Plettl, R. E. Brenner and P. Ziemann, *Biomaterials*, 2013, **34**, 8851–8859.
- 38 T. A. Owen, M. Aronow, V. Shalhoub, L. M. Barone, L. Wilming, M. S. Tassinari, M. B. Kennedy, S. Pockwinse, J. B. Lian and G. S. Stein, *J. Cell. Physiol.*, 1990, **143**, 420–430.